Available online at www.sciencedirect.com
ScienceDirect
Nuclear Instruments and Methods in Physics Research A 577 (2007) 168–172
NUCLEAR INSTRUMENTS & METHODS IN PHYSICS RESEARCH Section A
www.elsevier.com/locate/nima

High-brightness heavy-ion injector experiments ☆

G.A. Westenskow[a,*], J.W. Kwan[b], D.P. Grote[a], F. Bieniosek[b]

[a]Lawerence Livermore National Laboratory, P.O Box 808, Livermore CA 94551, USA
[b]Lawerence Berkeley National Laboratory, 1 Cyclotron Rd., Berkeley, CA 94720, USA

Available online 23 February 2007

Abstract

To provide a compact high-brightness heavy-ion beam source for Heavy Ion Fusion, we have performed experiments to study a proposed merging beamlet approach for the injector. We used an RF plasma source to produce the initial beamlets. An array of converging beamlets was used to produce a beam with the envelope radius, convergence, and ellipticity matched to an electrostatic quadrupole channel. Experimental results were in good quantitative agreement with simulation and have demonstrated the feasibility of this concept. The size of a driver-scale injector system using this approach will be several times smaller than one designed using traditional single large-aperture beams. The success of this experiment has possible significant economical and technical impacts on the architecture of HIF drivers.

PACS: 07.77.Ka; 41.85.Ar; 29.27.Ac

Keywords: Ion source; Particle injector; RF plasma source; Emittance

1. Introduction

Following a proposal that the usual limits on brightness for compact ion-beam sources used in Heavy Ion Fusion can be circumvented by using a multi-beamlet injector [1], we have performed a series of experiments to examine practical issues.

The final source envisioned will start with 200 5-mA beamlets across a 100-kV gap. The beamlets will be focused by Einzel Lens while their energy is increased to about 1.2 MeV. The beamlets are then merged to produce a 1-A beam with a normalized $4*\mathrm{rms}$ emittance of about $1\,\pi$-mm-mrad at 1.6 MeV. For the envisioned source we need low-temperature ions that can provide ion emission densities of $\sim 100\,\mathrm{mA/cm^2}$ of Ar^+, and an accelerator/focusing system where the maximum electrical fields are $\sim 100\,\mathrm{kV/cm}$. The main beam transport issues involved in the multi-beamlet approach are emittance growth and envelope matching in the merging process.

We first performed an experiment with an RF Plasma source to create the beamlets. Section 2 will briefly describe the results. Next, to accelerate/focus the beamlets we used an Einzel Lens Array. To ensure that we can hold the design voltage gradients in the source environment we performed the Full Gradient Experiments described in Section 3. Finally, the scaled merging experiments described in Section 4 was performed. Our goal was to confirm the emittance growth and to demonstrate the technical feasibility of building a driver-scale HIF injector.

2. Individual beamlets

We used an RF plasma source to produce our argon ion beamlets. The plasma chamber had a 26-cm inner diameter with multicusp permanent magnets to confine plasma. RF power (13.6 MHz) was applied to the source via a 2-turn, 11-cm diameter porcelain coated antenna inside the chamber. The RF power was typically applied for about 400 μs while the accelerating gap voltage was typically applied on for 20 μs. We have shown that we can extract

☆This work has been performed under the auspices of the US DOE by UC-LBNL under contract DE-AC03-76SF00098 and by UC-LLNL under contract W-7405-ENG-48, for the Heavy Ion Fusion Virtual National Laboratory.

*Corresponding author.
E-mail address: westenskow1@llnl.gov (G.A. Westenskow).

0168-9002/$ - see front matter © 2007 Elsevier B.V. All rights reserved.
doi:10.1016/j.nima.2007.02.050

100 mA/cm^2 from the chamber. Optimum performance at 80 kV was achieved with ~2 mTorr gas in the plasma chamber using 22 kW of RF drive power. The lowest emittance (best optics) was achieved when the beamlet current was slightly below the peak current value. Current density was found to increase with RF power as long as there was sufficient extraction voltage. At 80 kV, we have reached our goal of producing 100 mA/cm^2 of Ar^+ ions (i.e. 4.9 mA per beamlet). For operation with 10 kW of drive power we estimated that less than 5% of the extracted ions were in the Ar^{++} state. The thermal temperature of the ions was below 1 eV. Additional details about the RF plasma source have been published [2,3].

3. Full Gradient Experiments

In order to prevent space charge blow-up, the beamlets must be kept separated and focused during pre-acceleration. The pre-accelerator made use of Einzel Lens focusing, and high voltage gradient, to handle the high current density beamlets. In this experiment, 61 beamlets were extracted from an RF-driven Ar^+ plasma source with current density up to 100 mA/cm^2.

The Full Gradient Experiment was designed to test the electrical gradient limit in the working environment of the RF Plasma source. The dimensions and electric fields are typical of what we would like to use in a driver scale injector. Since we were limited to about 400-kV of pulsed voltage, only the first five gaps of a full system could be tested (See Fig. 1). In this experiment, the beam current is "full-scale".

For these experiments we tested a 61-beamlet extraction array using a series of Einzel lens. To reduce the fabrication cost we did not use curved plates. The highest vacuum electric field gradient occurred between the 2nd plate and the 3rd plate, and was 100 kV/cm on axis for a 1.2 cm gap. Fields at the edge of the holes were expected to be about 120 kV/cm for the experiment. The source apertures were 2.2 mm in diameter while all the other electrodes had 4.0 mm diameter holes. The current per beamlet was 3.8 mA, and the extraction current density was 100 mA/cm^2. There were 61 beamlets for a total current of 232 mA.

One of our goals was to test the high gradient insulators (HGI) which were used to assemble the electrode plates. When tested individually, each would hold 80 kV DC without beam. The insulators were either 4.27 cm or 2.13 cm in length. A conservative working voltage is about 30 kV/cm for a 20 μs pulse in the gap environment. Achieving these gradients required conditioning of the surfaces.

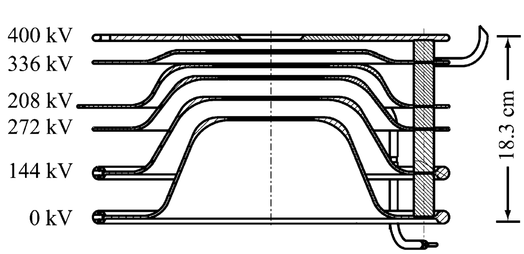

Fig. 1. Side view of the electrodes used in the Full Gradient Experiment. Electric Field between the 2nd and 3rd plate was 100 kV/cm.

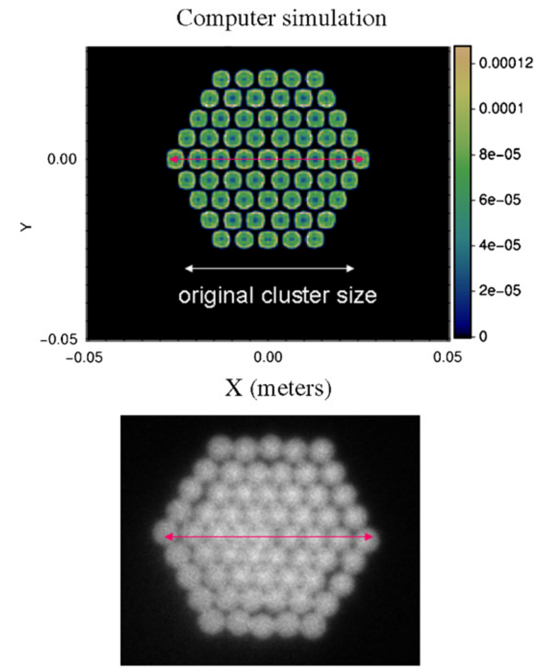

Fig. 2. Simulation and measured beamlets for the full gradient experiment at the exit of the Einzel lens array. The arrows are 16 cm long.

Fig. 2 shows the measured beam images at exit of the bottom plate and the corresponding simulation prediction. Here the beamlets have not been fully merged and therefore the image shows the current density uniformity across the array.

In trying to reach 400 kV with this module, we encountered a voltage breakdown problem at the last gap. Since, this gap has a lower design voltage gradient than the second gap which held voltage, we concluded that the problem was most likely due to a defective insulator. By shorting the final gap we were able to reach full current operation.

4. Merging beamlets

The main physics issues for merging beamlets are envelope matching and emittance growth in the merging process. For a proof-of-principle test of the merging process we have designed an experiment at full dimensions, but which will operate at one-quarter the voltage of a drive scaled injector. According to the Child–Langmuir electrostatic scaling law ($I \sim V^{3/2}$), the beam current will be reduced to $\frac{1}{8}$. Since all the voltages in this electrostatic system are reduced by the same factor, and the current density is scaled according to the "$\frac{3}{2}$" space charge limited condition, the beam optics of merging remains unchanged. Design of the system used the WARP-3D computer code [4].

Since the front end of an HIF induction linac uses electrostatic quadrupoles (ESQ) for beam transport, it is desirable to produce an elliptically shaped beam spot at the ESQ channel entrance to eliminate the conventional ESQ matching section. There are two ways to do this matching: (1) start with a circular array of beamlets and focus the $x-z$ and $y-z$ planes differently (astigmatic), or (2) start with an elliptical array of beamlets and focus the transverse planes equally. Although the first way was preferred because having the same initial $x-x'$ and $y-y'$ emittance could reach equilibrium quicker, we found that electrodes curved differently in the two planes were too expensive to make so we used the second method instead.

The emittance growth (normalized to a constant beam current) is minimized when the beamlet energy is high (at the time of merging), the number of beamlets is large, and the beamlets are close to each others. The final emittance depends on the initial beamlet convergent angle and weakly on the ion temperature [1]. Fig. 3 shows the simulated evolution of beamlets in $x-z$ configuration space. The x and y rms emittance was found to initially rise to different values because of the elliptical shape but later came to an equilibrium value (average between x and y emittance) in about 10 m distance.

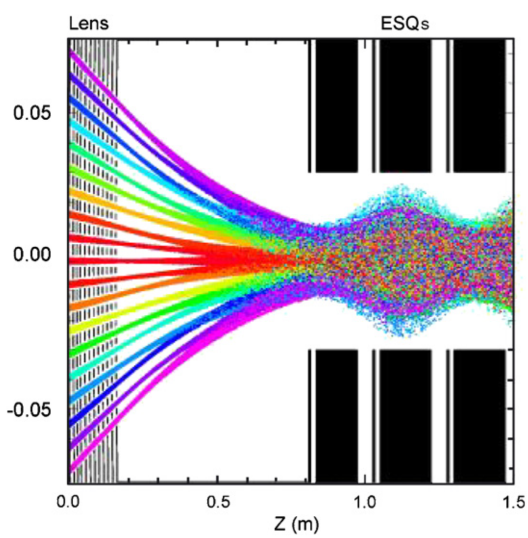

Fig. 3. Simulated particle trajectories in x-z space. The quadrupole fields in the experiment were different that what was used to generate the figure.

4.1. Experimental hardware

A layout of the experimental hardware is shown in Fig. 4. In this experiment 119 multi-beamlet were merged into a beam. On the left was a RF-driven multicusp ion source. Next was the Einzel Lens Array that had 12 electrodes, and was glued together using HGIs. These electrodes were curved with a common focal point just before the first ESQ entrance. Voltages were tapped from the grading rings of the voltage-grating column that surrounded the hardware. Fig. 5 shows the lens assembly mounted in the column and Fig. 6 shows a typical curved plate in the lens assembly with 119 apertures. Because the voltages between plates was reduced by a factor of four, we did not need reentrant cups, as in the Full-Gradient Experiment. We used HGI directly between the plates to hold the assemble together and provide alignment.

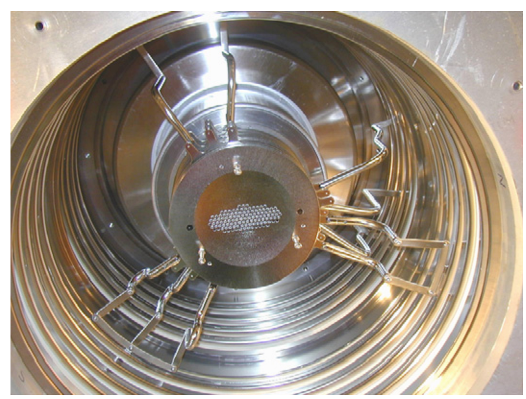

Fig. 5. Einzel lens assemble for the merging experiment installed in the top of the column (without the field shield installed).

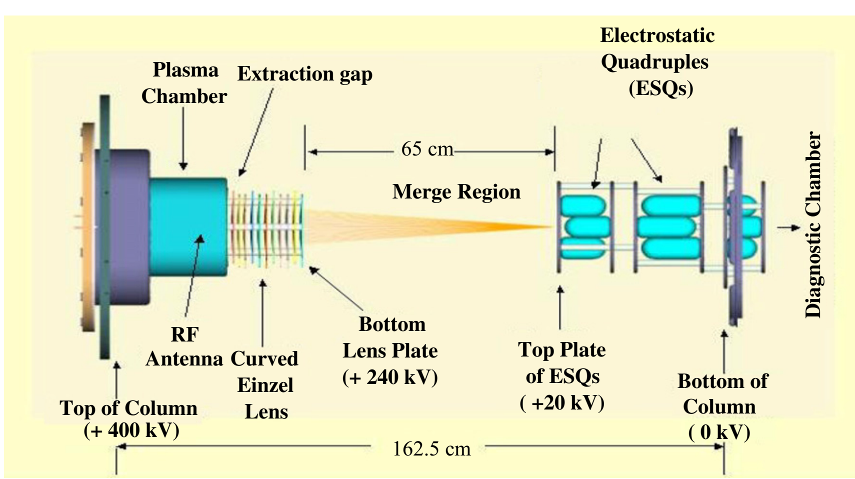

Fig. 4. Layout of the merging beamlet experiment.

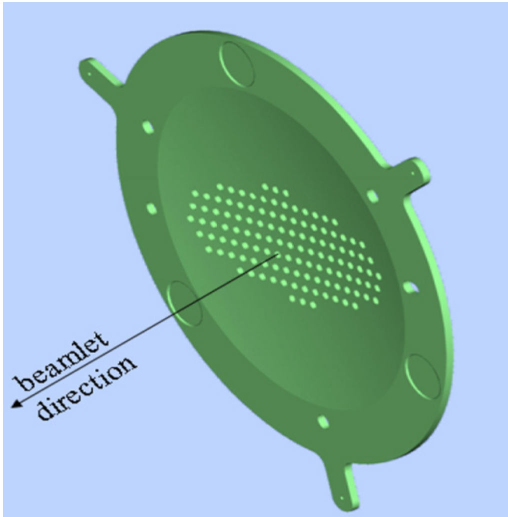

Fig. 6. One of the lens plates with 119 beamlet holes. The radius of curvature is about 60 cm.

4.2. Experimental results from the merging beamlets experiment

We measured the beam's emittance after the beamlets were merged and passed through the ESQ. Our goal was to confirm the emittance growth and compare the current profiles with simulation. Fig. 7 shows a typical $x - x'$ phase-space diagram taken at 10 cm after the exit. The scan was done using an ''optical scanner'' that had a front slit with a scintillator imager at the back. Although the beamlets are merged together into a large beam, the fine features in the diagram reveal the reminiscence of original beamlets. Fig. 8 shows an emittance diagram from simulation. Data from the optical scanner and from conventional double-slit scanner were both agreeing with that from simulation. We also had good agreement between the double-slit scanner $y - y'$ emittance data and simulation (but not the optical scanner in this direction which had poor resolution). Signal noise made it difficult to find the edge of the phase space in the experiments. The optical emittance scans used a 90% amplitude cutoff. For the slit scanner data, we plotted the emittance vs. cutoff level, fit a line to the data in the 70–90% cutoff region, then reported the line's intercept at the 100% level. The simulations line is the $4 * \text{rms}$ emittance taken for 90% of the ions.

The unnormalized emittance as a function of beam voltage is plotted in Fig. 9. The unnormalized emittance does not depend on the injector voltage if the perveance is held constant and the focusing fields are scaled to the beam voltage. The main contribution to the phase area was the ''trapped'' area when the beamlets were merged.

Fig. 10 shows the beam current into the Faraday cup as a function of the beam voltage. The simulation beam current assumes a flat emitting meniscus. Higher current can be obtained at the expense of inferior beam optics if the ion-emitting surface are allowed to bulge into the extraction gap by overdriving the RF plasma. At near 400 kV we believe that we were losing current from gas collision near the Faraday Cup. Obtaining good transport required that we operated near the correct perveance. At 400 kV we measured 70 mA into the Faraday Cup. Scaling this result up to the full voltage of 1.6 MV for a driver-scale injector, the full beam current would be $8 \times 70\,\text{mA} = 560\,\text{mA}$.

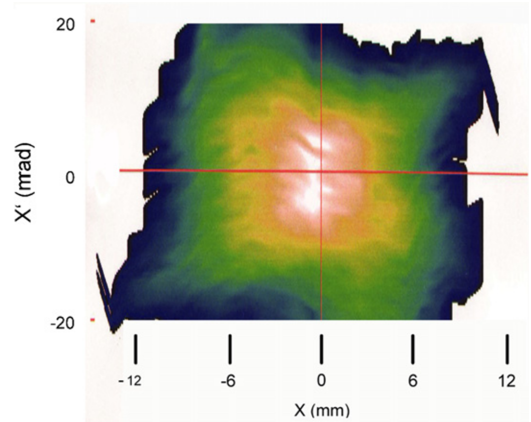

Fig. 7. Optical measurement of $x - x'$ phase space at 10 cm below the last quadrupole.

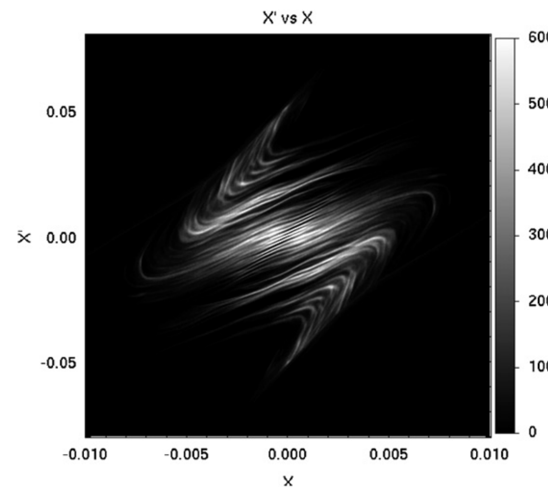

Fig. 8. Simulation of the $x - x'$ phase space at 10 cm below the last quadrupole. Horizontal scale is in meters, and the vertical scale is in radians.

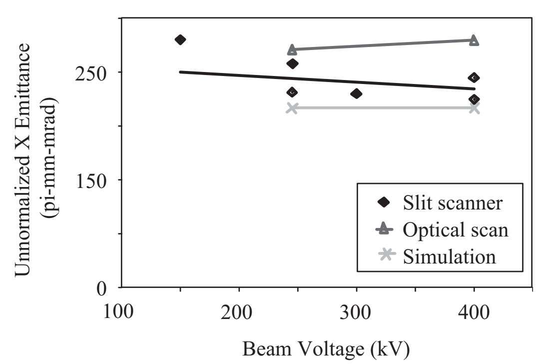

Fig. 9. Comparison of the measured unnormalized x emittance and the same emittance predicted by simulation.

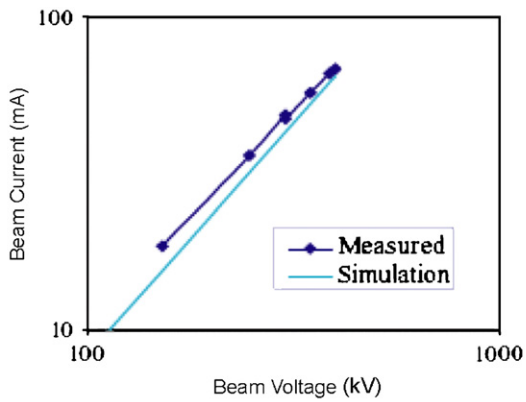

Fig. 10. Beam current into Faraday cup located after the ESQs.

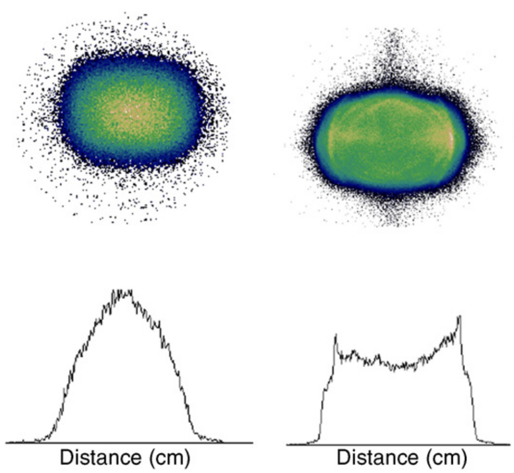

Fig. 11. Profile of the merged beam after the first ESQ and 10 cm after the third ESQ. The vertical edge width is about 4 cm for both sets.

Using alumina scintillators, we produced optical images of the beam's cross-section at two different locations: first at the beginning of the second ESQ, and then at 10 cm after the exit of the ESQ channel. These images are shown in Fig. 11. The first image was taken without applying ESQ voltages in order to observe the beam condition right after merging but before ESQ focusing. The second image showed the beam condition after going through the ESQ transport channel. These data confirmed that the 119 beamlets had merged to form an elliptically shaped beam. Fine structures in the current density were caused by the original discrete beamlets and should dissipate to form a homogenously uniform beam as the beam propagates further downstream.

5. Summary

In an 80-kV 20 – μs experiment, the RF plasma source has produced up to 5 mA of Ar^+ in a single beamlet. An extraction current density of $100\,mA/cm^2$ was achieved, and the thermal temperature of the ions was below 1 eV. We have tested at full voltage gradient the first four gaps of an injector design. Einzel lens were used to focus the beamlets while reducing the beamlet-to-beamlet space charge interaction. We were able to reach greater than 100 kV/cm in the first four gaps. We also performed experiments on a converging 119 multi-beamlet source. Although the source has the same optics as a full 1.6 MV injector system, these tests were carried out at 400 kV due to the test stand HV limit. Experimental results were in good quantitative agreement with simulation and have demonstrated the feasibility of this concept.

Acknowledgements

We would like to thank Gary Freeze, Robert Hall, Erni Halaxa, and Will Waldron for their assistance with the experiments. Larry Ahle led the construction stage of the test stand. We would also like to thank Grant Logan, Alex Friedman, John Barnard, and Christine Celata for their constant encouragement.

References

[1] D.P. Grote, E. Henestroza, J.W. Kwan, Phys. Rev. ST Accel. Beams 6 (2003) 014202.
[2] J.W. Kwan, et al., Nucl. Instr. and Meth. A 544 (2005) 134.
[3] G.A. Westenskow, et al., Nucl. Instr. and Meth. A 544 (2005) 436.
[4] D. Grote, et al., Design and Modeling of the Multibeamlet Injector, these proceedings, submitted for publication.